Submillimeter Guided-Wave Experiments with Polyethylene Slab Waveguides

MIKIO TSUJI, STUDENT MEMBER, IEEE, KUNITAKA KAWAI, HIROSHI SHIGESAWA, MEMBER, IEEE, AND KEI TAKIYAMA, MEMBER, IEEE

Abstract—**The attenuation constants of a symmetric polyethylene slab waveguide are measured in the submillimeter-wave region at $\lambda_0 = 337$ μm. In our experiments the fine metal grating is used as a coupler, instead of a usual prism coupler. Our coupler which is different from the conventional grating coupler fixed on a slab is easily movable along a slab without a fluctuation in the coupling efficiency, and the loss measurement is successfully performed for several kinds of slab thicknesses by using such couplers. As a result, the attenuation constant of about 1.3 dB/m is measured, in good reliability, for a slab of 10 μm in thickness.**

Finally, to make clear the accuracy of our loss measurements, the transverse broadening of the field along the propagating direction of a slab is measured experimentally, and it is concluded that there is little influence of the transverse broadening on the measured attenuation constants.

I. Introduction

RECENTLY, microwave and optical techniques have become more sophisticated and many of these techniques can be extended to the submillimeter-wave region. As for the guided-wave techniques in this wavelength range, several types of waveguiding structures have been investigated [1]–[9]. One of the important waveguides for most applications will be a dielectric stripline [10]. However, there is now the biggest difficulty in finding the low-loss dielectric materials in the submillimeter-wave region, and such a stripline has not yet developed.

In this paper, we have studied the transmission characteristics of dielectric slab waveguides as the basic guide form of a dielectric stripline. The attenuation constant is one of the most significant parameters for estimating the applicability of this guide for the submillimeter-integrated circuits. Tacke *et al.* [8] have measured the attenuation constant of a polyethylene slab waveguide by varying the distance between the two prism couplers, and Danielwicz *et al.* [9] have done the same experiment by using a crystal quartz as the slab. However, in such a type of coupler based on the frustrated total reflection, the power coupling to a slab waveguide is so sensitive to a gap between a slab and a prism that it is practically impossible to keep up the constant coupling of a movable prism over the sufficient length for loss measurements. It is evident that the accuracy of loss measurements is perfectly owing to this constant coupling, and then the "sliding metal grating coupler" has been proposed to perform such measurements with sufficient accuracy and reliability. In this paper, we have measured the attenuation constants of a symmetric polyethylene slab waveguide by using this grating coupler, and obtained the attenuation constant of 1.3 dB/m for the TM_0 mode with 10-μm thickness.

Finally, since a slab waveguide provides confinement of the field in only one dimension, the transverse broadening of a guided wave has been measured to show the accuracy of our loss measurements, and it has been concluded that this broadening has negligible effects on our measured attenuation constants.

Manuscript received January 29, 1979; revised June 12, 1979.

The authors are with the Department of Electronics, Doshisha University, Kyoto 602, Japan.

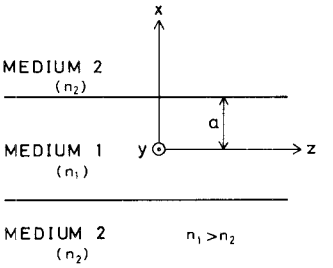

Fig. 1. Schematic diagram of a symmetric slab waveguide.

II. Theoretical Considerations

A dielectric slab waveguide of thickness $2a$ is shown schematically in Fig. 1. The slab is assumed to have refractive index n_1 and is embedded in an infinite medium with refractive index n_2. By considering the infinite extent of the slab in both y and z directions, the field can be decomposed into TE and TM modes and each of them should satisfy the boundary conditions independently.

As mentioned before, the present slab waveguide in the submillimeter-wave region will be always constructed with a lossy dielectric and all of the constituent variables of the eigenvalue equation become complex quantities. To solve such a complex eigenvalue equation, Burke [11] has shown an interesting method in which an eigenvalue equation is transformed into two simultaneous equations. These equations are given in the Appendix where the general expression applicable to all modes is derived instead of the limited one in [11].

Now, in our experiments, the refractive index n_2 is assumed to be real and unity (air), while the dielectric slab

0018-9480/79/1100-0873$00.75 ©1979 IEEE

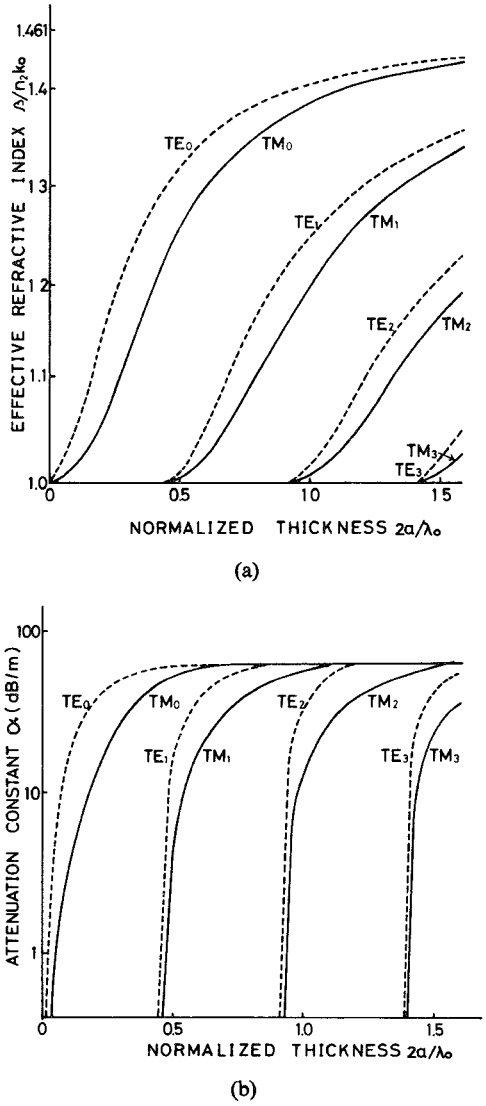

Fig. 2. Complex propagation constant h for various modes as a function of the normalized thickness $2a/\lambda_0$. (a) Phase constant. (b) Attenuation constant.

is assumed to be a polyethylene film of which refractive index at $\lambda_0=337$ μm becomes the complex value $n_1=1.461-j0.000387$ by reference to the optical constant [12]. Thus a graphical method [11] is available to solve such a complex eigenvalue equation.

Consequently, the calculated results of the phase constant β and the attenuation constant α for each propagating mode are shown as a function of the normalized slab thickness $2a/\lambda_0$ in Fig. 2(a) and (b), where the effective refractive index β/n_2k_0 is employed instead of β.

In the following sections, these results will be used successfully to explain the experimental results.

III. Experiments

A. Sliding Metal Grating Coupler and Its Characteristics

In the first step of experiments, the selective launching of each propagating mode has been studied. It is well known to use a prism [8] or a grating coupler [9] for this purpose. Especially the former can be applicable to measure the attenuation constant of a slab waveguide by moving it along a slab. However, in such a type of coupler based on the frustrated total reflection, the power-coupling efficiency is so sensitive to a gap between a slab and a prism that it is practically impossible to keep up the constant coupling of a movable prism over the sufficient length for loss measurements. It is evident that the accuracy of loss measurements is perfectly owing to this constant-coupling efficiency, and then the sliding metal grating coupler has been designed to perform the loss measurements with sufficient accuracy and reliability.

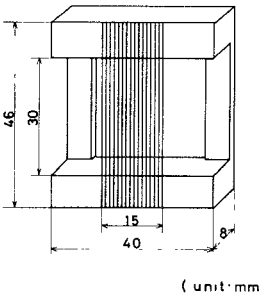

Fig. 3. Basic structure of the sliding metal grating coupler.

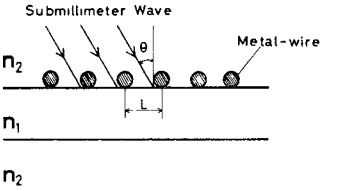

Fig. 4. Side view of a metal grating coupler having a period L. The submillimeter wave is launched with the angle θ.

The structure of our grating coupler shown in Fig. 3 is different from the conventional grating coupler fixed on a slab, and the fine metal wires are fixed periodically on the rigid frame. Unlike a prism coupler, our grating coupler provides the desirable behavior when the grating is mounted with a slight pressure to realize a close contact with the slab. In a grating coupler, the period of the grating L is related to the angle of incidence θ of the laser beam onto the metal grating through the following phase-matching condition (see Fig. 4):

$$\beta_m = k_0 \sin\theta + \frac{2\pi}{L} n \tag{1}$$

where β_m is the propagation constant of mth guided mode in a dielectric slab waveguide and n is the order number of diffraction. Considering both the use of an HCN laser ($\lambda_0=337$ μm) and the backward-wave coupling with $n=-1$ to excite selectively a guided mode, (1) yields a reasonable period of 200 μm for the practical grating. Fig. 5(a) is the photograph of our handmade coupler in which the Molybdenum wires of 100 μm in diameter are arranged with the period of 200 μm, as shown in Fig. 5(b).

Now, to investigate the characteristics of our grating

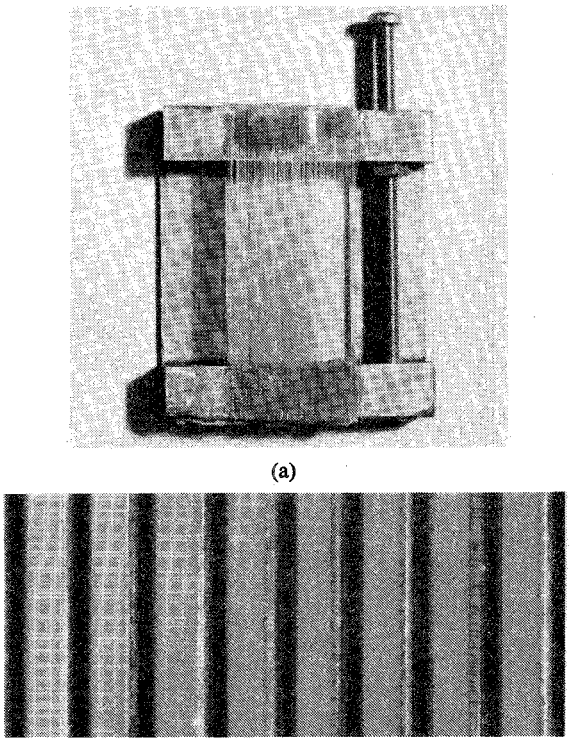

(a)

(b)

Fig. 5. Photographs of (a) the handmade grating coupler, and (b) the Molybdenum wires (100 μm in diameter) arranged with the period of 200 μm.

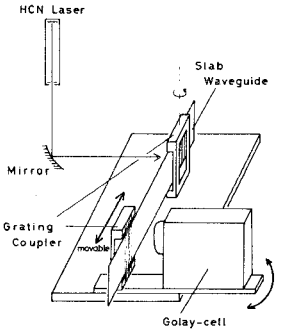

(a)

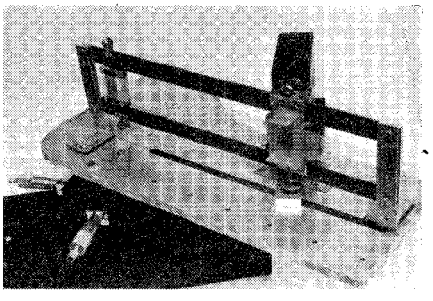

(b)

Fig. 6. (a) Illustration of experimental setup. (b) Its external view.

coupler, the experimental setup shown in Fig. 6(a) are employed, where the thin polyethylene film of size 3×30 cm^2 is used as a slab and is fully stretched in practice over

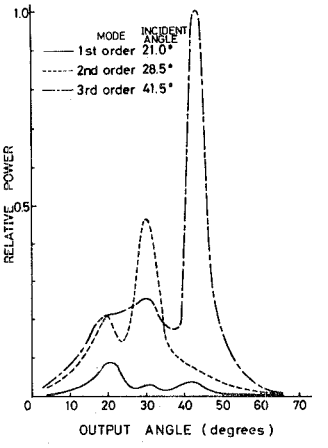

Fig. 7. Behavior of the sliding metal grating coupler in the selective excitation of each propagating mode.

TABLE I
MEASURED[1] AND THEORETICAL LAUNCHING ANGLES

Mode number	Theoretical values		Mesured values	
			Incident angle	Output angle
0	TE 14.3°	TM 14.7°		
1	19.5°	21.1°	21.0°	20.5°
2	28.6°	31.4°	28.5°	30.0°
3	41.3°	42.2°	41.5°	42.5°

[1]In this measurement, the propagation of the zeroth-order mode is confirmed, but its measured angle is eliminated because its attenuation is too great to measure the launching angle accurately.

a metal frame, as shown in Fig. 6(b). Two sliding metal grating couplers are mechanically contacted on its surface so that the beam from an HCN laser can be coupled into and out of the guide. The laser beam focused by spherical mirror has an approximately Gaussian cross section with an e^{-2} power diameter of 1 cm. As shown in these figures, the slab waveguide and both couplers are mounted on a rotary stage which allows to vary the angle of incidence θ_{in} of the laser beam onto the input grating coupler.

On the other hand, a Golay cell detector is mounted on the rotatable arm in the output side so as to measure the direction θ_{out} of an output beam peculiar to each guided mode. The distance between Golay cell detector and the grating coupler is 40 mm and the aperture of Golay cell detector is 1 mm in diameter.

Here, the output power is measured by varying the angle θ_{out} when the angle θ_{in} is fixed to excite one of guided modes. The results for the polyethylene slab of 500 μm in thickness are shown in Fig. 7. Although the eight modes can propagate in this guide, the maximum output is obtained at the output angle θ_{out} nearly equal to the angle of incidence of θ_{in} of the launched mode, and hence, we may conclude that little mode conversion occurs through propagation. The relations between these angles (θ_{in} and θ_{out}) are summarized in Table I to compare with the theoretical angles calculated from (1). It is clear from this Table that the measured angles are in good agreement

with calculated ones and each guided mode can be selectively launched and detected by our grating couplers.

Of course, the launching angles for the TE_n mode and TM_n mode are close each other, and owing to little difference between them it is hard to distinguish them. However, it is reasonable to conclude the predominant launching of the TM modes in our experiments because there will be high reflection at the metal grating coupler for the TE incident wave with the electric-field vector parallel to the metal wires, and also the attenuation constant of a slab waveguide is higher for the TE mode than for the TM mode. Although more detailed studies about our grating coupler should be performed, the coupling efficiency of about 40 percent may be attained in its maximum.

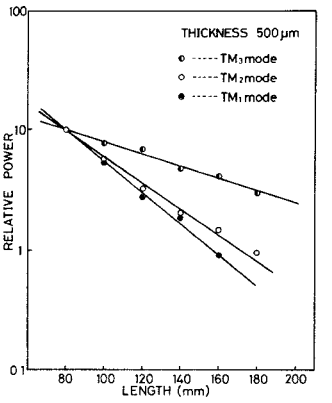

Fig. 8. Loss measurements for various modes in the slab waveguide with 500-μm thickness. (Relative output powers are measured as a function of its length.)

B. Measurements of Attenuation Constant

The sliding metal grating coupler discussed in the previous section is very useful for the measurement of attenuation constant. The attenuation constant of a dielectric slab waveguide is measured by moving the output coupler along a slab and varying the transmission length of modes. The experimental setup is the same as that in Fig. 6, except that both the output grating coupler and the rotatable arm on which Golay cell detector is mounted are movable along a slab simultaneously.

Typical results are shown in Figs. 8 and 9. In Fig. 8, the relative output power for various modes in the slab waveguide with 500-μm thickness are shown as a function of the length of a guide. Then the attenuation constant is found as 130 dB/m for the TM_1 mode, 110 dB/m for the TM_2 mode, and 52 dB/m for the TM_3 mode. These measured values are found to be about twice as much as the theoretical ones denoted in Fig. 2(b).

So far, the multimode slab waveguide has been discussed. Now, let us examine a thin slab waveguide in which only the fundamental modes (the TE_0 and TM_0 modes) can propagate. As seen from Fig. 2(a), such a waveguide can be realized for the slab thickness less than about 160 μm at $\lambda_0 = 337$ μm, and then the attenuation constants for the TM_0 mode are measured for several kinds of slab thicknesses (100 μm, 50 μm, 35 μm, and 10 μm). All these results are obtained in the same accuracy as that in Fig. 8, and are plotted in Fig. 9 as a function of the slab thickness.

It is noted from this figure that the measured results have shown a relatively good agreement with the calculated ones indicated by the solid line, and the attenuation of 1.3 dB/m is obtained for the TM_0 mode with 10-μm thickness. As seen from this figure, the measured values are slightly greater than the calculated ones. This difference may be caused by the radiation losses due to irregularities and inhomogeneities in a waveguide and also by the underestimation of the loss tangent, $\tan\delta$, of a polyethylene in the calculation, since the commercial polyethylene often involves the various impurities having much effects upon its absorption in the submillimeter-wave region [12].

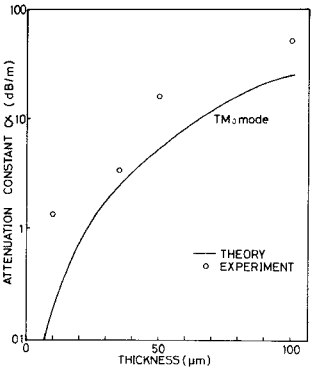

Fig. 9. Attenuation constant for the TM_0 mode.

C. Effects of the Transverse Broadening of the Field on the Measured Attenuation Constants

A dielectric slab waveguide provides confinement of the field in only one dimension, i.e., the x direction in Fig. 1. Thus to make the accuracy of our loss measurements in the previous section more clear, we should prove that the transverse broadening of the untrapped field in the y direction has no influences upon the measured attenuation constants, even though the guide length, i.e., the distance between the input and output couplers, becomes over 300 mm. So this transverse broadening of the field is measured along the propagating direction of a slab waveguide by means of two simple methods.

In the first method, the output power is measured when a small submillimeter-wave absorber (3 mm^2 in area) is put on the surface of a slab and is moved along the transverse direction. Such a measurement is performed at the three positions l mm far from the input coupler ($l = 30$, 100, and 200 mm). The results are shown in Fig. 10(a) as a function of the displacement of the absorber from the center of a slab. It is clear from these results that the half-width of the power dip caused by the absorber coin-

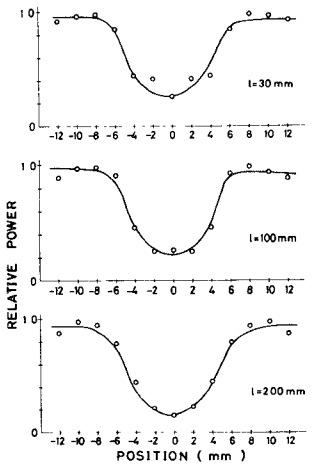

(a)

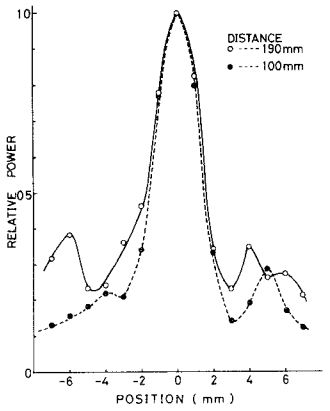

(b)

Fig. 10. Measurements of the transverse broadening of the field. (a) Output powers are measured when a small absorber is moved on the surface of a slab waveguide. (b) Intensity distributions of the near field radiated from the end of a slab waveguide are measured by scanning a detector.

cides with that of the input beam (i.e., about 10 mm), and there are little variations with increasing l.

In the second method, the near-field pattern of radiation from the end of a slab waveguide is measured by scanning the Golay cell detector along the transverse direction of a slab. In this experiment, the distance between the input coupler and the end of a slab is adjusted to 100 mm and 190 mm, and the near-field pattern is measured at the distance of 50-mm apart from the end of a slab. The result shown in Fig. 10(b) indicates that the transverse broadening of the input beam remains with little variation in its half-width over the transmission range of about 200 mm.

Consequently, it is proved from these results that the field of a guided wave is so well confined to a polyethylene slab in 30-mm width that its side edges have no effect upon the propagation of a guided mode. Thus as for the length of a slab used in our measurement, it may be concluded that the transverse broadening of the field has negligible effects on the measured attenuation constants.

IV. Conclusion

The attenuation constant of symmetric slab waveguides is measured by using the sliding metal grating coupler in the submillimeter-wave region. As a result, the attenuation constant for the TM_0 mode is found, in good reliability, to be as low as 1.3 dB/m for a slab of 10 μm in thickness. Also, it is confirmed that the transverse broadening of the field along the propagating direction of a slab has little influence on the measurement of the attenuation constant. However, the polyethylene slab waveguide of which thickness is as thin as about 10 μm, confines only the transmission energy of less than 10 percent in the polyethylene, and so the radiation losses due to the bends must be considered. Moreover, the coupling efficiency of the sliding metal grating coupler should be estimated precisely. These problems will be discussed in the following papers.

Appendix
Eigenvalue Equations with Complex Constituent Variables

The waveguiding structure shown in Fig. 1 has a plane of symmetry in the y–z plane, and the propagating modes may then be classified roughly by both symmetric and antisymmetric ones. Following to the notations employed in [13], the well-known eigenvalue equations are shown as follows:

$$q = \eta u \tan u, \qquad \text{for the symmetric modes} \tag{A-1}$$

$$q = -\eta u \cot u, \qquad \text{for the antisymmetric modes} \tag{A-2}$$

where u and q are the normalized wavenumbers in the x direction of mediums 1 and 2, respectively, and

$$\eta = \begin{cases} 1, & \text{for the TE mode} \\ n_2^2/n_1^2, & \text{for the TM mode.} \end{cases} \tag{A-3}$$

Then the properties of eigenmodes propagating along the z axis can be derived from these equations, in conjunction with the conservation relation of wavenumbers:

$$u^2 + q^2 = (n_1^2 - n_2^2)k_0^2 a^2 \equiv R^2 \tag{A-4}$$

where k_0 is the free-space wavenumber and the propagation constant h in the z direction is given by

$$(ha)^2 = (n_1 k_0 a)^2 - u^2 = (n_2 k_0 a)^2 + q^2. \tag{A-5}$$

Substituting (A-4) into (A-1) and (A-2), we then have

$$u^2(1 + \eta^2 \tan^2 u) = R^2, \qquad \text{for the symmetric modes} \tag{A-6}$$

and

$$u^2(1 + \eta^2 \cot^2 u) = R^2, \qquad \text{for the antisymmetric modes.} \tag{A-7}$$

When the lossy dielectric slab is concerned, the constituent variables of (A-6) and (A-7), i.e., u and η and R^2 become complex ones, say, $u = u' + ju''$. In this case, it is convenient to indicate R^2 in terms of its magnitude M and argument ϕ as follows:

$$R^2 = Me^{j\phi}. \tag{A-8}$$

Substituting (A-8) into (A-6) and (A-7), each of those eigenvalue equations are transformed into two simultaneous equations for u' and u'', and these can be shown independently of modes as follows:

$$M = (u'^2 + u''^2)\cdot\sqrt{m_r^2 + m_i^2} \tag{A-9}$$

$$\phi = \tan^{-1}\left(\frac{2u'u''}{u'^2 + u''^2}\right) + \tan^{-1}\left(\frac{m_i}{m_r}\right) \tag{A-10}$$

where m_r and m_i are given as follows:

$$m_r = \{(\cos 2u' \pm \cosh 2u'')^2 + (\eta'^2 - \eta''^2)(\sin^2 2u' - \sinh^2 2u'') \mp 4\eta'\eta'' \sin 2u' \sinh 2u''\}/(\cos 2u' \pm \cosh 2u'')^2 \tag{A-11}$$

$$m_i = 2\{\eta'\eta''(\sin^2 2u' - \sinh^2 2u'') \pm (\eta'^2 - \eta''^2) \sin 2u' \sinh 2u''\}/(\cos 2u' \pm \cosh 2u'')^2. \tag{A-12}$$

The upper sign holds for the symmetric modes, while the lower sign holds for the antisymmetric modes. Simultaneous equations (A-9) and (A-10) may be solved graphically by plotting both contours of equal magnitude and argument, as shown in [11].

References

[1] H. Shigesawa, M. Tsuji, K. Kawai, and K. Takiyama, "Transmission of submillimeter waves in dielectric waveguides," presented at the Third Int. Conf. on Submillimeter Waves and Their Applications, SB1.3, 1978.

[2] K. Yamamoto, "Analysis of gas confined dielectric waveguides," in *paper Tech. Group on Microwaves*, IECE of Japan, MW77-53, pp. 51–58, July 1977.

[3] K. Takiyama and H. Shigesawa, "Experimental study of *H*-guide transmission characteristics in millimeter (50-Gc) wave region," *Sci. Eng. Rev.* Doshisha Univ., vol. 2, pp. 139–150, Mar. 1962.

[4] R. J. Batt, H. L. Bradley, A. Doswell, and D. J. Harris, "Waveguide and open-resonator techniques for submillimeter waves," *IEEE Trans. Microwave Theory Tech.*, vol. MTT-22, pp. 1089–1094, Dec. 1974.

[5] T. Yoneyama and S. Nishida, "Oversize single-mode *H*-guide," *Electron. Lett.*, vol. 14, pp. 148–149, Mar. 1978.

[6] H. Shigesawa and K. Takiyama, "Transmission characteristics of the close grooved guide," *J. Inst. Electron. Commun. Eng. Jap.*, vol. 50, pp. 114–121, Nov. 1967.

[7] D. J. Harris, K. W. Loe, and J. M. Reeves, "Waveguide system for short-millimetric and submillimetric wavelengths," presented at IEEE MTT-S Int. Microwave Symp., C6-3, June 1978.

[8] M. Tacke and R. Ulrich, "Submillimeter waveguiding on thin dielectric films," *Opt. Commun.* vol. 8, pp. 234–238, July 1973.

[9] E. J. Danielwitz and P. D. Coleman, "Far-infrared guided wave optics experiments with anisotropic crystal quartz waveguides," *IEEE J. Quantum Electron.*, vol. QE-13, pp. 310–317, May 1977.

[10] B. Senitzky and A. A. Oliner, "Submillimeter waves—a transition region," in *Proc. Symp. Submillimeter-Waves*, Polytechnic Press of Polytechnic Institute of Brooklyn, NY, 1970.

[11] J. J. Burke, "Propagating constants of resonant waves on homogeneous isotropic slab waveguides," *Appl. Opt.*, vol. 9, pp. 2444–2452, Aug. 1970.

[12] G. W. Chantry, J. W. Fleming, P. M. Smith, M. Cudby, and H. A. Willis," Far infrared and millimeter-wave absorption spectra of some low-loss polymers," *Chem. Phys. Lett.*, vol. 10, pp. 473–477, Aug. 1971.

[13] N. S. Kapany and J. J. Burke, *Optical Waveguide*. New York: Academic, 1972.

The Edge-Guided Mode Nonreciprocal Phase Shifter

DONALD M. BOLLE, SENIOR MEMBER, IEEE, AND SALVADOR H. TALISA, MEMBER, IEEE

***Abstract*—Results of a theoretical study are presented for a four-region model of a nonreciprocal dielectric–ferrite loaded stripline phase shifter employing the edge-guided dynamic mode. The behavior of our model in terms of the differential phase shift, the insertion loss, and the effective bandwidth is explored as a function of the various parameters involved.**

Manuscript received September 25, 1978; revised June 15, 1979.

The authors are with the Division of Engineering, Brown Univeristy, Providence, RI 02912.

I. Introduction

ONE OF THE fundamental structures which support the edge-guided mode is a ferrite loaded stripline with the dc magnetic biasing field oriented normal to the ground plane. This geometry was introduced by Hines [1] who explored the possibilities of obtaining broad-band nonreciprocal isolation and phase shifting. These two

0018-9480/79/1100-0878$00.75 ©1979 IEEE